# CHAPTER 21

## RANDOM WAVE SIMULATION IN A LABORATORY WAVE TANK

Akira Kimura

Research Assistant

and

Yuichi Iwagaki

Professor

Department of Civil Engineering
Kyoto University
Kyoto, Japan

ABSTRACT

Most of coastal engineering problems have been studied with monocromatic waves. However, sea waves which arrive at the coast are random. It is very difficult to estimate exactly the influence of these random waves to coastal structures. Then the model tests in a laboratory wave tank using random wave simulation techniques seem to be most desirable way to estimate the influence of randomness of sea waves. For this purpose, the accomplishment of random wave simulation system, which make possible generating random waves having statistically same properties as those of sea waves, has long been desired. The authors achieved to establish such a new wave simulation system. In this paper, the characteristics of this system are demonstrated experimentally through several cases of random wave simulations.

## INTRODUCTION

Random wave simulations are usually perfomed with a random wave generator in a laboratory wave tank. Then the important problem is how to drive the random wave generator to simulate random sea waves. In other words, how to generate random signals by which the random wave generator is driven becomes important. There are two ways of generating random signals, classifying random wave simulation techniques roughly. One is an analog method and the other is a digital method. In both methods, we must define at first what kind of properties of random waves should be simulated. Power spectrum shapes, Gaussian distribution of the water surface elevation and Rayleigh distribution of the wave height are well known representative properties for random sea waves. Simulated random signals must have the above properties at least. Especially the power spectrum shape of the simulated random signal must be same as that of sea waves.

It is known experimentally that other properties besides the power spectrum shape are almost same as those of sea waves if the power spectrum shape of simulated random waves is similar to that of sea waves. So the main purpose of random wave simulation is how to simulate the power spectrum shape of sea waves.

The analog method is the electrical simulation technique using band-pass filters. Random noise generated electrically is transmitted into a band-pass filter unit which is consist of many band-pass filters with slightly different central frequencies. Gains of each filter are controlled so as to make equal the power of the output signal from each filter to the initially specified function in each frequency band. This initially specified function will be called as a target spectrum. Output signals from each filter are superimposed each other. Then the power spectrum of the output signal becomes equal to the target spectrum consequently. Finally this signal is transmitted into the random wave generator (1),(2).

The digital method is usually carried out by means of a digital computer. Random numbers generated by the computer are averaged using a numerical filter with a weighted moving average method. Averaged values are converted into analog record by a D-A converter and transmitted into the random wave generator. In this method, the procedure for designing the numerical filter mathematically, which transforms random numbers to random signals of specified properties, becomes important. Usually this problem can be deduced to solving Wiener-Hopf's integral equation, which is necessary and sufficient conditions that input and output signals must satisfy. But this procedure is very complicated and laborious and there is no assurance of the existence of an analytical solution in any case (3),(4).

From the fundamental knowledge about the Fourier transformation theorem, the numerical filter can be calculated easily by the reverse Fourier transformation of a linear spectrum. This numerical filter does not satisfy Wiener-Hopf's equation. In spite of mathematical discrepancy this method has been used frequently for convenience (5),(6),(7).

Beside these numerical filter methods, the wave superposition method has been treated by Borgman (5) and Goda (8). This is the most simple method to simulate random waves. But the simulated random waves by this method repeat themselves periodically every certain time interval. In order to avoid this periodicity several methods have been examined. Goda (8) recomended that the number of component waves is more than fifty. However, it can be said that when the number of component waves becomes so large it takes more time to calculate random signals than by the numerical filter method.

The authors propose herein a new method to calculate numerical filters. The procedure of this method is very simple and the numerical filter obtained satisfies Wierner-Hopf's equation.

## NUMERICAL FILTER

The problem to obtain a numerical filter can be deduced to design mathematically an optimum circuit system which transforms a white noise $x(t)$ to a random wave profile $y(t)$ of desired statistical properties. In Fig.1 showing a linear circuit system, $h(\tau)$ and $g(\tau)$ mean unit impulse response functions in the normal and reverse directions of the circuit respectively. The relations between $x(t)$ and $y(t)$ are expressed as

$$y(t)=\int_0^\infty h(\tau)\ x(t-\tau)\ d\tau \cdots\cdots\cdots\cdots (1)$$

$$x(t)=\int_0^\infty g(\tau)\ y(t-\tau)\ d\tau \cdots\cdots\cdots\cdots (2)$$

Eqs.(1) and (2) can be written as follows in digital form expressions:

$$y_t=\sum_{\tau=0}^{\infty} h_\tau\, x_{t-\tau} \cdots\cdots\cdots\cdots (3)$$

$$x_t=\sum_{\tau=0}^{\infty} g_\tau\, y_{t-\tau} \cdots\cdots\cdots\cdots (4)$$

where $x_t$, $y_t$, $h_\tau$, $g_\tau$, $x_{t-\tau}$ and $y_{t-\tau}$ are digitized values of x(t), y(t), h(τ), g(τ), x(t-τ) and y(t-τ) with a time interval dτ. Substituting Eq.(4) into Eq.(3) gives

$$y_t=\sum_{\tau=0}^{\infty} h_\tau \sum_{n=0}^{\infty} g_n\, y_{t-n-\tau}=\sum_{\tau=0}^{\infty} h_\tau \sum_{n=-\infty}^{t-\tau} g_{t-\tau-n}\, y_n$$

$$=\sum_{n=-\infty}^{t} y_n \sum_{\tau=0}^{t-n} g_{t-n-\tau}\, h_\tau \cdots\cdots\cdots\cdots (5)$$

Then from the condititon that $y_t$ appearing in both sides of Eq.(5) are always equal, the following relation is derived:

$$\sum_{\tau=0}^{t} g_{t-\tau}\, h_\tau=\delta_t \quad (t=0,\ 1,\ 2,\cdots\cdots\infty) \cdots\cdots\cdots (6)$$

where $\delta_t$ is Dirac delta function

$$\delta_t=1\ (t=0),\quad \delta_t=0\ (t\neq 0) \cdots\cdots\cdots\cdots (7)$$

In Eq.(6), if either $h_\tau$ ( $\tau$ = 0,1,2, .... ,∞ ) or $g_\tau$ are known, the other can be determined easily. But $h_\tau$ and $g_\tau$ are not yet defined independently. Then other conditions are introduced to define $h_\tau$ and $g_\tau$ separately. In Eqs.(3), (4) and (6), it is impossible to sum up infinitely in real computation, then the upper boundary of summation is replaced by a sufficientely large number N . Now the white noise having the following characteristics is introduced newly as a random input:

$$E[x_t]=0,\quad E[x_t\, x_{t-\tau}]=\delta_\tau \cdots\cdots\cdots\cdots (8)$$

where E[ ] means time averaging procedure.

If it is assumed that $h_\tau$ ( $\tau$ = 0,1,2, .... ,N ) are given, $g_\tau$ are known from Eq.(6). $y_t$ ( t = 0,1,2, .... ,∞ ) can be determined by substituting the white noise $x_t$ into Eq.(3). Newly defined white noise $x'_t$ obtained by substituting these $y_t$ into Eq.(4) must be equal to $x_t$, but there are little differences between them, because the upper value of the summation is replaced by a sufficiently large but finite number N in Eqs.(3),(4) and (6). Then let us try to obtain $h_\tau$ and $g_\tau$ which will minimize the mean squares of the difference between $x_t$ and $x'_t$.

$$D^2=E[(x_t-x_t')^2]=E[x_t^2]-2E[x_t x_t']+E[x_t'^2] \quad \cdots\cdots(9)$$

From Eqs.(3), (4) and (8) and the condition $h_i = 0$ when $i < 0$, Eq.(9) can be written as

$$D^2=1-2\sum_{\tau=0}^{N} g_\tau \; E[x_t y_{t-\tau}] + \sum_{\tau=0}^{N}\sum_{n=0}^{N} g_\tau g_n r_{\tau-n}$$
$$=1-2h_0 g_0 + \sum_{\tau=0}^{N}\sum_{n=0}^{N} g_\tau g_n r_{\tau-n} \quad \cdots\cdots(10)$$

where $r_i$ ( i = 0,1,2, .... , N ) are digital values of the autocorrelation function of the output $y_t$. In order to obtain $g_i$ ( i = 0,1,2, .... , N ) which minimize $D^2$, differentiating Eq.(10) with respect to $g_i$ and putting each equation to be equal to zero, the following equation can be derived:

$$\sum_{\tau=0}^{N} g_\tau r_{\tau-n}=h_0\delta_n \; (n=0,\ 1,\ 2,\cdots N) \quad \cdots\cdots(11)$$

This equation can also be expressed in matrix representation as

$$\begin{pmatrix} r_0 & r_1 & r_2 \cdots\cdots r_N \\ r_1 & r_0 & r_1 \cdots\cdots r_{N-1} \\ r_2 & r_1 & r_0 \cdots\cdots r_{N-2} \\ \multicolumn{3}{c}{\cdots\cdots\cdots\cdots} \\ r_N & r_{N-1} & r_{N-2} \cdots r_0 \end{pmatrix} \begin{pmatrix} g_0 \\ g_1 \\ g_2 \\ \vdots \\ g_N \end{pmatrix} = \begin{pmatrix} h_0 \\ 0 \\ 0 \\ \vdots \\ 0 \end{pmatrix} \quad \cdots\cdots(12)$$

As $h_0$ appearing in the right hand side of Eq.(12) is still unknown, then an attempt to solve the equations except the top ones including $h_0$ is made. This means to solve the matrix of rank N-1.

$$\begin{pmatrix} r_0 & r_1 & r_2 \cdots\cdots r_{N-1} \\ r_1 & r_0 & r_1 \cdots\cdots r_{N-2} \\ r_2 & r_1 & r_0 \cdots\cdots r_{N-3} \\ \multicolumn{3}{c}{\cdots\cdots\cdots\cdots} \\ r_{N-1} & r_{N-2} & r_{N-3} \cdots r_0 \end{pmatrix} \begin{pmatrix} g_1/g_0 \\ g_2/g_0 \\ g_3/g_0 \\ \vdots \\ g_N/g_0 \end{pmatrix} = - \begin{pmatrix} r_1 \\ r_2 \\ r_3 \\ \vdots \\ r_N \end{pmatrix} \quad \cdots(13)$$

Now denote the solution of this matrix by $g'_i$ ( i = 1,2, .... , N ), which are the ratios of $g_i$ to $g_0$ as seen in Eq.(13).

Putting n = 0 in Eq.(11) gives

$$g_0 r_0+g_1 r_1+g_2 r_2+\cdots\cdots+g_N r_N=h_0 \quad \cdots\cdots(14)$$

If both sides of Eq.(14) are devided by $g_0$, Eq.(14) is written as

$$r_0+g_1'r_1+g_2'r_2+\cdots\cdots+g_N'r_N=h_0/g_0 \quad \cdots\cdots(15)$$

The left hand side of Eq.(15) can be determined by solving Eq.(13). Denoting the total summation of Eq.(15) by q , $g_n$ can be expressed as follows:

$$g_n=\frac{h_0}{q}g_n' \quad \cdots\cdots(16)$$

Substituting these relations into Eq.(10), the following equation can be obtained:

$$D^2=1-\frac{h_0^2}{q} \quad \cdots\cdots(17)$$

If q is possitive, $D^2$ has a minimum value zero when $h_0^2 = q$ . From Eq.(16), $g_n$ can be finally determined as

$$g_0=\frac{1}{\sqrt{q}},\quad g_n=\frac{g_n'}{\sqrt{q}}(n=1,\ 2,\cdots\cdots N)\cdots\cdots(18)$$

Substituting these $g_n$ into Eq.(6), then $h_n$ ( n = 0,1,2, .... , N ) can be determined. $h_n$ are the numerical filters which transforms the white noise into random signals of a target spectrum.

## NUMERICAL SIMULATION

In this section numerical simulations using the method explained previously are treated, and the results are compared with target spectra.

In addition random wave simulations by the Fourier transformation method are compared with those by this method. Two types of numerical filters can be defined by the Fourier transformation method. One is a numerical filter and the other is an asymmetrical one. From the results of numerical simulations in the preceding study, it was found that the asymmetrical filter gives better results than the symmetrical one. Then the results of random wave simulations by the newly proposed method herein will be compared with those by the asymmetrical filter.

Random signals by the Fourier transformation method are calculated by the relation

$$y_t = \sum_{i=-N/2}^{N/2} a_i \cdot x_{t-i} \quad \cdots\cdots\cdots (19)$$

where $a_i$ ( i = -N/2, .... ,0, .... , N/2 ) are the numerical filters defined by the sine transformation of a linearized target spectrum. Eq.(19) has a similar form to Eq.(3) except lower limit of the summation.

The spectrum for random sea waves is frequently expressed as

$$S(f)=c_1 f^{-m}\exp(c_2 f^{-n}) \quad \cdots\cdots(20)$$

where $c_1$, $c_2$, m and n are constants determined by wave conditions. This equation can be normalized using the peak frequency $f_p$ and the spectral value $S(f_p)$ as follows:

$$S(f)=S(f_p)(f/f_p)^{-m} \cdot\exp\left\{\frac{m}{n}[1-(f/f_p)^{-n}]\right\} \qquad \cdots\cdots\cdots\cdots(21)$$

Values of $f_p$ and $S(f_p)$ used in this numerical simulation are tabulated in Table-1. Target spectra are determined by substituting these values into Eq.(21). Autocorrelation functions are calculated by Wiener-Khintchine's theorem.

By substituting the digitized autocorrelation function into Eqs.(6), (13), (15) and (18), numerical filters can be determined. Fig-2 shows the examples of the numerical filters tabulated in Table-1. These numerical filters transform the random numbers, which have flat characteristics of power spectrum density, into the random signals of a target spectrum.

Fig-3 shows a part of uniform random numbers used in these numerical simulations. These random numbers are generated by the mixed congruence method using the computer subroutine. Fig-4 shows a part of numerically simulated random waves in Case-I-b.

Fig-5(a)∿(d) and Fig-6(a)∿(f) show the plots of the power spectra of simulated random waves by the proposed method and the Fourier transformation method (dotted lines) with the target spectra (solid lines). It is known from these figures that the proposed method gives better results than the Fourier transformation method.

These numerical simulations were perfomed in same conditions. N in Eq.(3) and Eq.(19) is 128 and the time interval $d\tau$ is 0.05 sec. So the same degree of accuracy can be obtained by this new method with a smaller value of N than by the Fourier transformation method.

Goda (8) concluded,based on his experimental study that the time interval $d\tau$ is preferable to satisfy the following relation:

$$d\tau \leq \frac{0.05}{f_p} \qquad \cdots\cdots\cdots\cdots\cdots (22)$$

This relation is satisfied in all cases. However, $d\tau$ must be selected not so as to be too little because when the time interval becomes small, N in Eq.(3) must he large. It is known from the accuracy of the simulated random waves that the moderate size of N is 100 or so and $d\tau$ is desirable to be equal to $0.05/f_p$ which is the largest value that satisfies Goda's criterion.

The numerical filters as shown in Fig-2 must satisfy the following Wiener-Hopf's integral equation which is necessary and sufficient conditions:

$$\psi_{xy}(\tau) = \int_0^\infty h(\sigma)\cdot\psi_x(\tau-\sigma)\, d\sigma \qquad (23)$$

where $\psi_{xy}$ is the crosscorrelation function between the input x(t) and the output y(t), $\psi_x$ is the autocorrelation function of the input x(t) and $h(\sigma)$ is the filter or weighting function.

This equation can be expressed in digital form as

$$E[\ x_{t-\tau}\cdot y_t\ ] = \sum_{\sigma=0}^{N} h_\sigma\cdot E[\ x_{t-\tau}\cdot x_{t-\sigma}\ ] \quad \ldots \quad (24)$$

The left hand side of Eq.(24) can be written using Eq.(3) as follows:

$$E[\ x_{t-\tau}\cdot \sum_{s=0}^{N} h_s\cdot x_{t-s}\ ] = \sum_{s=0}^{N} h_s\cdot E[\ x_{t-\tau}\cdot x_{t-s}\ ] \quad (25)$$

This is equal to the right hand side of Eq.(24). Therefore, $h_\tau$ ( $\tau$ = 0,1, 2, .... , N ) satisfy Wierner-Hopf's integral equation.

## RANDOM WAVE SIMULATION SYSTEM

Fig-7 shows the flow chart of the random wave simulation system. Two types of information can be available as an input of this system. One is a theoretical expression of the power spectrum or autocorrelation function. The other is the power spectrum or autocorrelation of observed sea waves or records of water surface itself. This system only needs basically the digitized autocorrelation function to simulate random waves. Either power spectra or autocorrelation functions can be available, because both are related each other by Wiener-Khintchine's theorem.

If the observed sea surface elevations are sellected as input of this system, the right hand side of this flow chart will be used. This part of the flow chart is mainly aimed to generate random numbers. Because it is a very difficult problem to determine the randomness of sea waves, this part is attached to introduce the randomness in the simulation procedure from the observed sea waves. Reverse numerical filter $g_\tau$ in Eqs.(4) and (6) are used to generate random numbers. Other procedures are the same as those at the left hand side of the flow chart.

Random waves in prototype must be reduced to a moderate size in order to generate in a laboratory wave tank. Usually the Froude similitude law is used to reduce the power spectra to a moderate scale. Then this reduced power spectrum will be called as a target spectrum. In the next step, the target spectrum must be modified because the random wave generator does not have flat response characteristics of frequency. Therefore, the wave making characteristics must be considered. In this system, Biesel-Suquet's theoretical relation between the movement of a wave making paddle and generated waves in a wave tank is adopted. Although this relation is for periodic small amplitude waves, it will be valid for random waves as the paddle movement is small. Fig-8 shows the experimental results for the ratio of the component amplitude of random waves to that of paddle movement. Plotted data agree well with the theoretical relations. Biesel-Suquet's theoretical relations shown in Fig-8 are expressed as

for piston type,

$$\frac{H}{2R} = \frac{2\sinh^2 kh}{\sinh kh \cosh kh + kh} \quad \ldots\ldots\ldots\ldots\ldots \quad (26)$$

for flatter type $\frac{H}{2R}=\frac{2\sinh kh}{kh}\cdot\frac{1-\cosh kh+kh\sinh kh}{\sinh kh\cosh kh+kh}$ (27)

The modified target spectrum S*(f) will be defined by

$$S^*(f)=S(f)\cdot[F(f)]^2 \qquad (28)$$

where S(f) is a target spectrum and F(f) the inverse expression of Eq.(26) or Eq.(27).

Pierson-Moskowitz and Neuman spectra are selected to demonstrate the feasibility of this system. Target spectra are determined by Eq.(21). $f_p$ and $S(f_p)$ of each spectrum are shown in Table-2. Fig-9 shows an example of the target spectrum and modified target spectrum.

Numerical filters were calculated in the same manner as used in the former section. Random numbers were averaged with the numerical filter, and these averaged values were transmitted into a D-A converter. The output signal from the D-A converter should be arranged to the smooth signal with the low pass filter. Then finally the random signals were transmitted into the wave generator.

Magnetic tapes and data recorders included in Fig-7 are attached to store digital and analog signals for future experiments.

Fig-10 shows the wave tank used in this system. This wave tank is 27 m long, 50 cm wide and 75 cm deep with glass side walls. At one end of this tank a random wave generator is furnished. At the other side of the wave tank, a wave absorver is installed and a wave gauge is set at the position of 10 m apart from the wave making paddle. Photo-1 and Photo-2 show the wave tank and random wave generator respectively.

The random wave generator is of servo-controlled electro-hydraulic system. Some typical properties of this wave generator are listed in Table-3. The wave generator has two actuators, which are connected with a piston type wave making paddle and a flatter type one respectively. Each actuator can be controlled independently. When the peak frequency of the target spectrum is higher than 1.0 Hz, random wave simulations will be perfomed with the flatter type wave making paddle, and if the peak frequency is lower than 1.0 Hz, the piston type wave making paddle is used. Furthermore, each paddle can be controlled simultaneously with different random signals.

A band pass filter unit not included in this system with fifteen band pass filters of 1/3 oct. frequency band from 0.2 to 5.0 Hz is attached as an optional faculty to this random wave generator. Therfor, the random wave simulations by an analog method can be made (2).

Fig-11 (a) ∿ (d) and Fig-12 (a) ∿ (d) show the experimental results of Pierson-Moskowitz and Neuman spectral simulations. The plotted data in each figure denote the results of power spectral analysis of water surface elevation measured by the wave gauge, and the solid lines show target spectra. From these figures, it is known that the power spectra of simulated waves are very close to the target spectra except in the region of low frequency.

The difference between the data and the target spectra at low frequency may be mainly caused by the surf beat which is usually observed in random waves near the coast.

This random wave simulation system aims to simulate a random wave spectrum. At the same time,other properties such as probability distributions of surface elevation and wave height must resemble those of sea waves.

Fig-13 shows some examples of the probability distributions of water surface elevation of simulated waves for Case-1-b and Case-2-a shown in Table-2. Plotted values are slightly skew to the minus side compared with the Gaussian distribution shown in a solid line, but this tendency is always observed in sea wave data. This is owing to the non-linear characteristics of wave motion.

Fig-14 shows wave height distributions defined by the zero-up-cross method for Case-1-b and Case-2-a. Agreement of data with the Rayleigh distribution is very well. These results means that the simulated waves in a wave tank have the same characteristics as those of sea waves.

## CONCLUSION

The random wave simulation system has been discussed with several cases of random wave simulations in a wave tank. New, simple and accurate method to determine the numerical filter in this system has been proposed. The numerical simulation of random waves and experiments in a laboratory wave tank have shown that this system is very satisfactory.

There are some restrictions of wave making in extremly low and high frequency regions not only for this system but also for a regular wave generator, even though the random wave generator adopted in this system is much improved so as to equipt two types of wave making paddles. It is, therefore very difficult to estimate random waves in wide frequency range, for example, random waves of widely separated multiple peaked spectrum by a usual random wave generator only.

The ideal random wave simulation system will be consist of an extremly low frequency random wave generator like a tsunami generator and an ordinary random wave generator and a wind tunnel.

This random wave simulation system was completed in 1973. Since then, more than 40 cases of random wave simulation have been perfomed, and the statistical characteristics of random waves,such as distributions of the wave period, wave height and wave period and also combined distributions, have been studied using these simulated random waves (9), (10)

REFERENCES

(1) Mohus,I. : Generation and measurement of simulated ocean waves, Automatic Control Laboratory, Norwegian Institute of Technology, Trondheim, pp. 1-32, 1960.
(2) Iwagaki,Y. and A.Kimura : A study on simulation of ocean waves by a random wave generator, Proc. 19th Conf. Coastal Eng. in Japan, pp.131-136, 1972. (in Japanese)
(3) Shvetsov,K.Y. and Shorin,A.N. : The modeling of sea waves by digital computer, Oceanology, Vol.9, pp.578-584, 1969.
(4) Hino,M. : A predictor filter and transformation filter for ocean waves (1), Proc. 14th Conf. Coastal Eng. in Japan, pp.21-28, 1967. (in Japanese)
(5) Borgman,L.E. : Ocean wave simulation for engineering design, Proc. ASCE, WW4, pp.557-583, 1969.
(6) Webber,N.B. and C.D.Christian : A programmable irregular wave generator, Proc. 14 th Conf. Coastal Eng., pp.340-351, 1974.
(7) Funke,R. : Random wave signal generation by minicomputer, Proc. 14th Conf. Coastal Eng., pp.352-371, 1974
(8) Goda,Y. : Numerical experiments on wave statistics with spectral simulation, Rpt. Port and Harbour Res. Inst. of Japan, Vol.9, pp.7-57,1970.
(9) Iwagaki,Y. and A.Kimura : A study on a characteristics of the period distributions of random sea waves, Proc. 22th Conf. Coastal Eng. in Japan, pp.295-300, 1975. (in Japanese)
(10) Iwagaki,Y. and A.Kimura : A study on a characteristics of zero-up-cross wave length and celerity, Proc. 23th Conf. Coastal Eng. in Japan, 1976. (in Japanese)

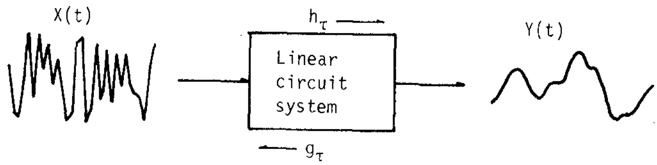


Fig-1 Diagram of linear circuit system

Table-1 Characteristics of target spectra

| Case No. | $f_p$ (Hz) | $S(f_p)$ | m | n | N |
|---|---|---|---|---|---|
| I -a | 0.6 | 1.0 | 4 | 4 | 128 |
| I -b | 0.6 | 1.0 | 5 | 4 | 128 |
| I -c | 0.6 | 1.0 | 6 | 4 | 128 |
| I -d | 0.6 | 1.0 | 7 | 4 | 128 |
| II -a | 0.4 | 1.0 | 5 | 4 | 128 |
| II -b | 0.6 | 1.0 | 5 | 4 | 128 |
| II -c | 0.8 | 1.0 | 5 | 4 | 128 |
| II -d | 1.0 | 1.0 | 5 | 4 | 128 |
| III -a | 0.8 | 1.0 | 5 | 4 | 64 |
| III -b | 1.0 | 1.0 | 5 | 4 | 64 |

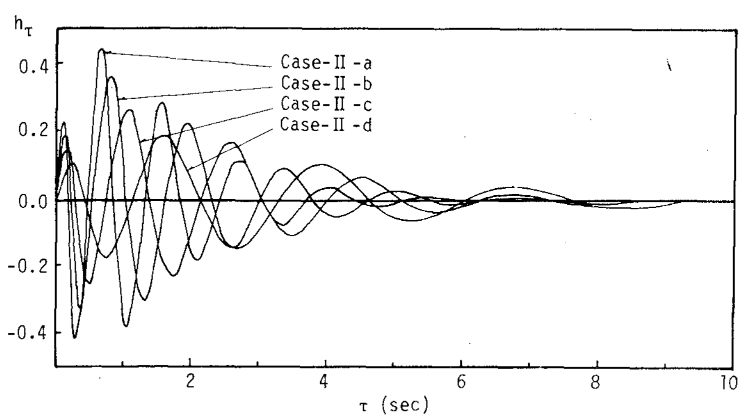


Fig-2 Examples of numerical filters

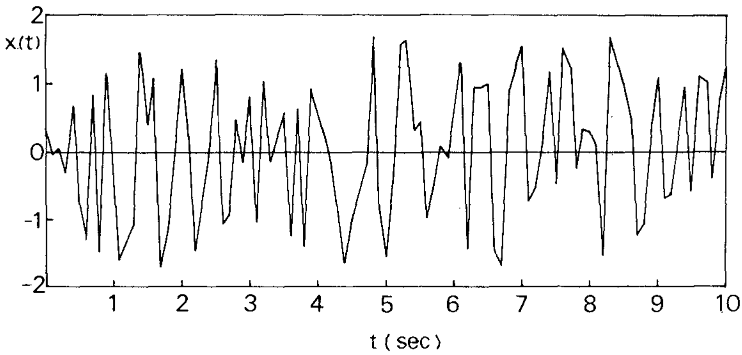


Fig-3 Uniform random numbers

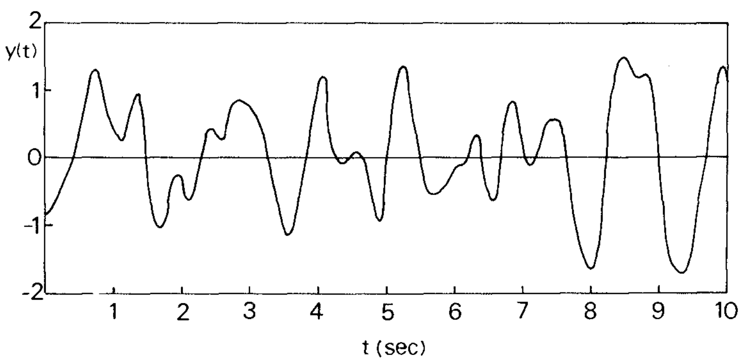


Fig-4 Signals of simulated waves ( Case-I-b )

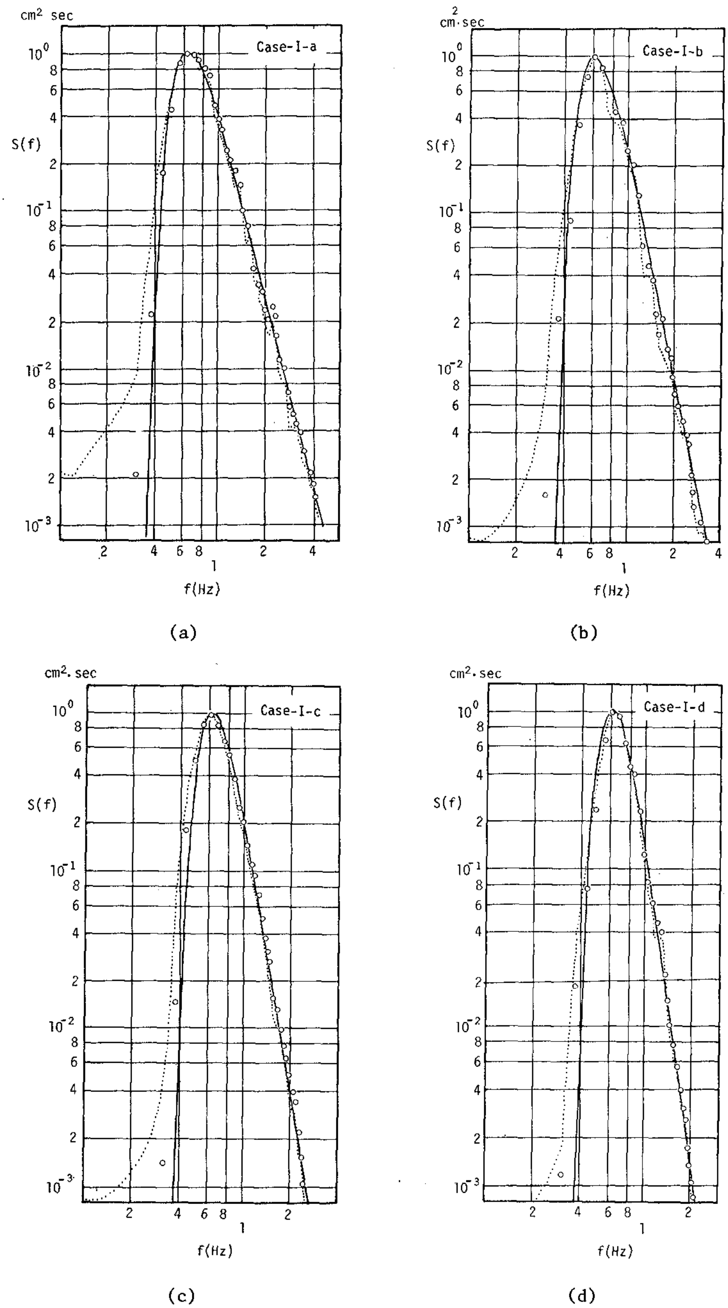


Fig-5 Power spectra of simulated waves ( Case-I )

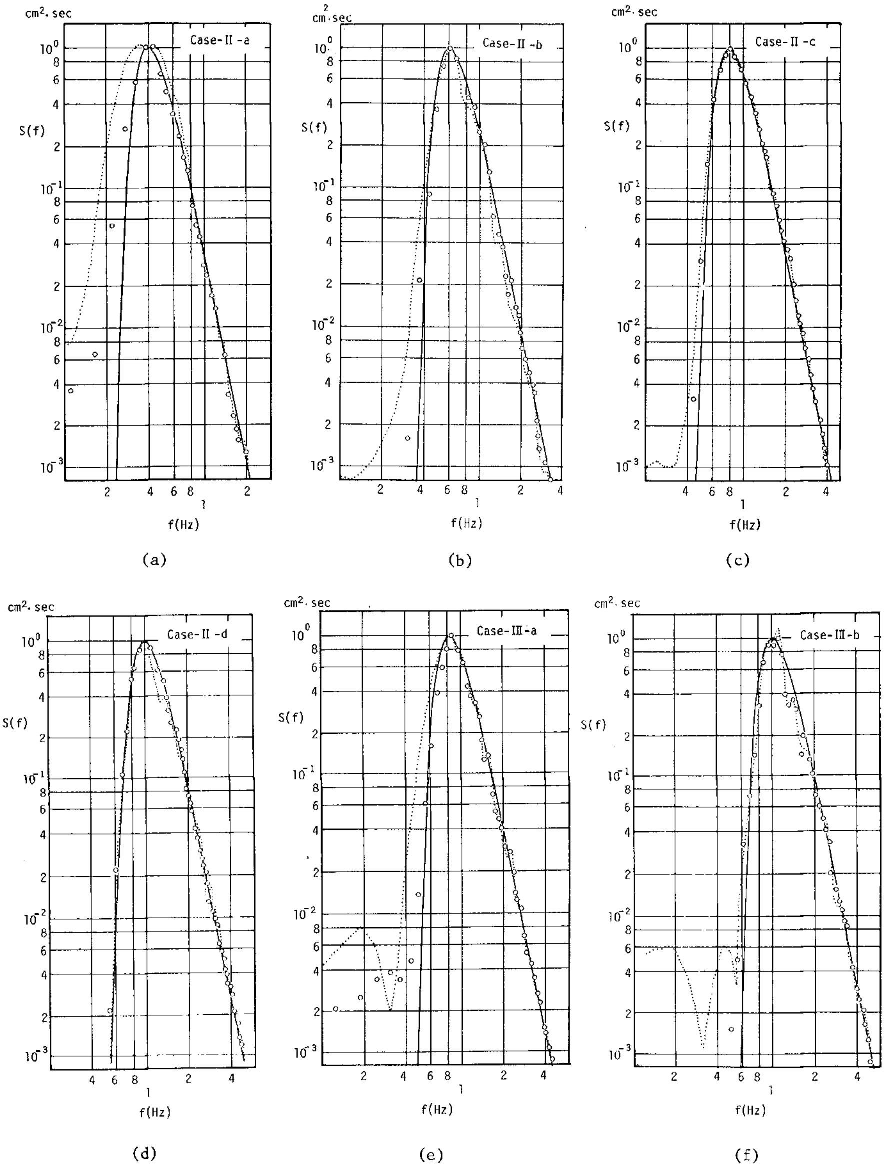


Fig-6 Power spectra of simulated waves ( Case-II and Case-III )

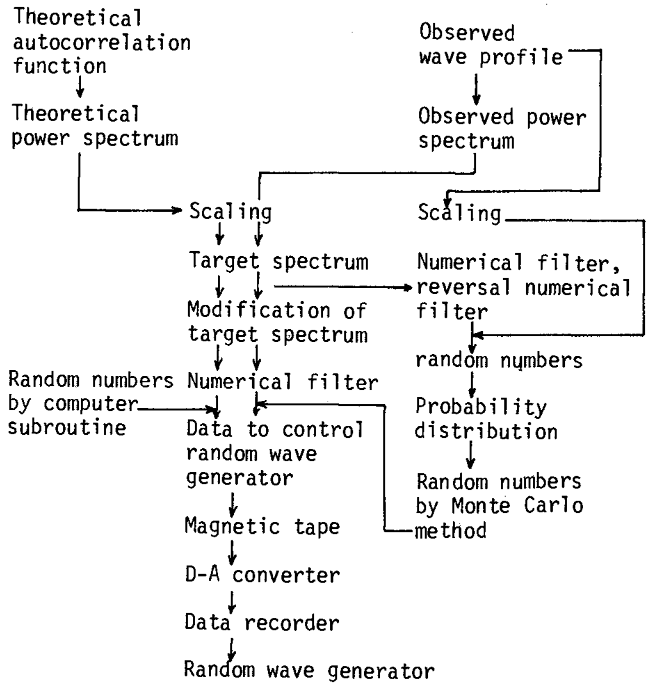


Fig-7 Flow chart of random wave simulation system

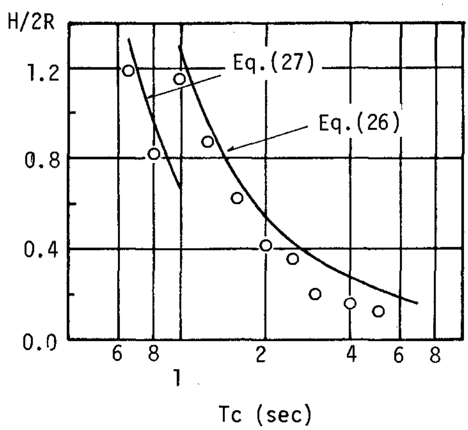


Fig-8 Period characteristics of wave generation by two types of wave paddles ( h=40 cm )

Table-2 Characteristics of target spectra used in experiments

| Case No. | $f_p$ (Hz) | $S(f_p)$ ($cm^2 sec$) | m | n |
|---|---|---|---|---|
| 1-a | 0.4 | 5.0 | 5 | 4 |
| 1-b | 0.5 | 5.0 | 5 | 4 |
| 1-c | 0.6 | 7.0 | 5 | 4 |
| 1-d | 0.7 | 10.0 | 5 | 4 |
| 2-a | 0.5 | 2.0 | 6 | 2 |
| 2-b | 0.6 | 2.0 | 6 | 2 |
| 2-c | 0.7 | 4.0 | 6 | 2 |
| 2-d | 0.8 | 5.0 | 6 | 2 |

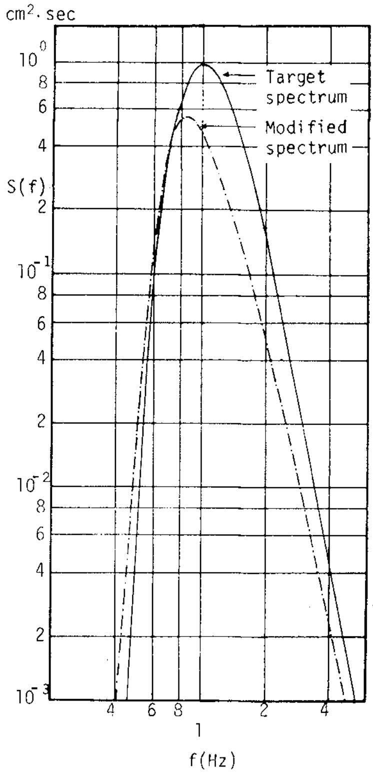


Fig-9 Target spectrum and Modified spectrum

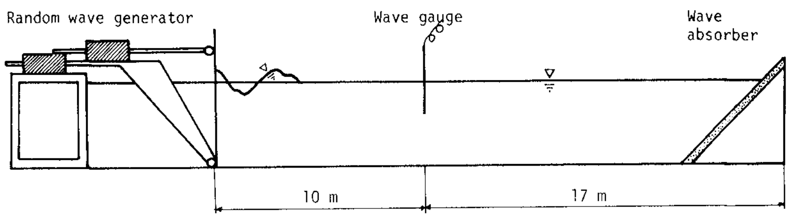


Fig-10 Wave tank

Photo-1 Wave tank

Photo-2 Random wave generator

Table-3 Typical properties of random wave generator

| | Maximum power | Maximum stroke | Frequency characteristics |
|---|---|---|---|
| Actuator (A) (Piston) | 1.0 ton | ± 10.0 cm | 0.01 ∿ 10.0 Hz |
| Actuator (B) (Flatter) | 0.5 ton | ± 10.0 cm | 0.01 ∿ 10.0 Hz |

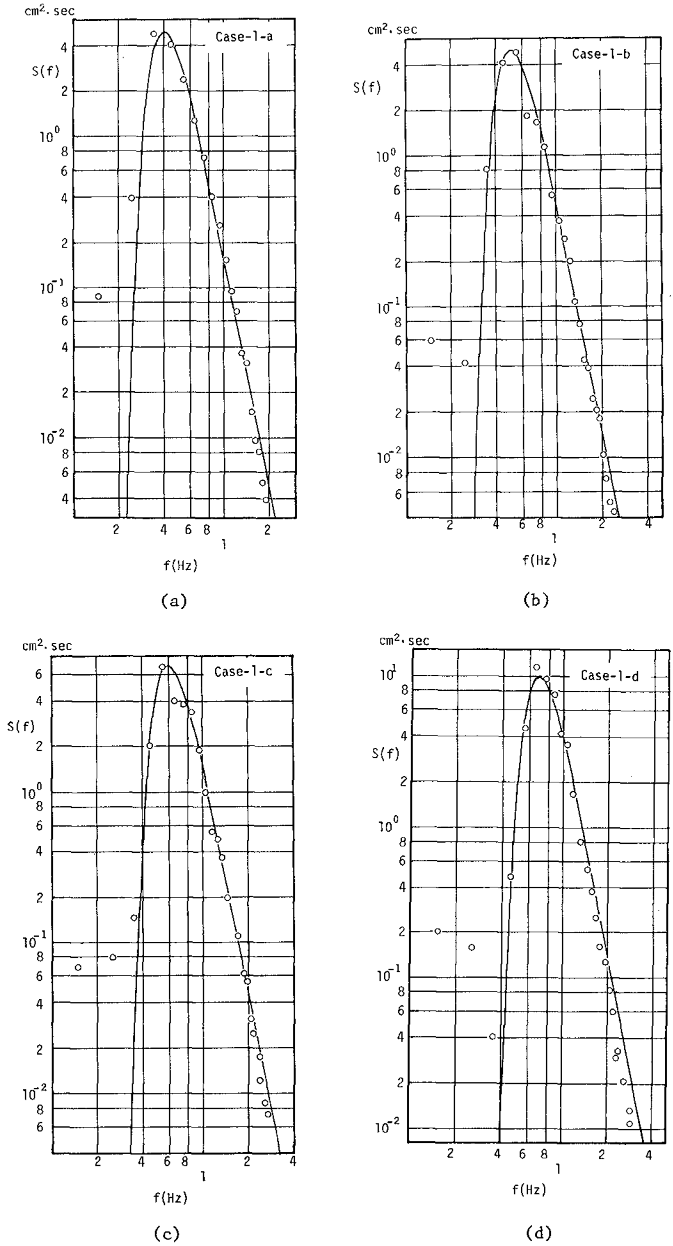


Fig-11 Power spectra of simulated waves in wave tank
( Pierson-Moskowitz spectra )

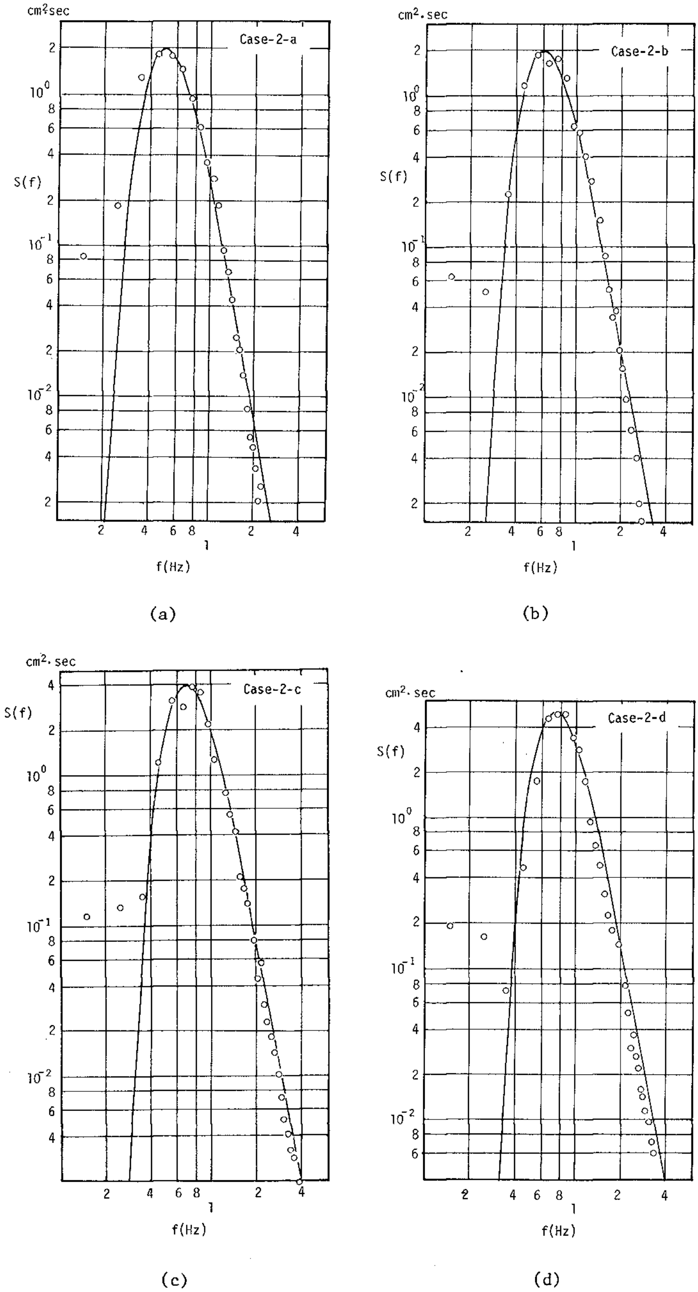


Fig-12 Power spectra of simulated waves in wave tank
( Neumann spectra )

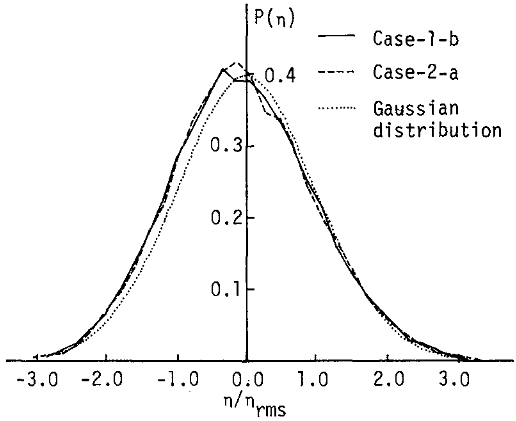


Fig-13 Probability distributions of water surface elevation of simulated waves

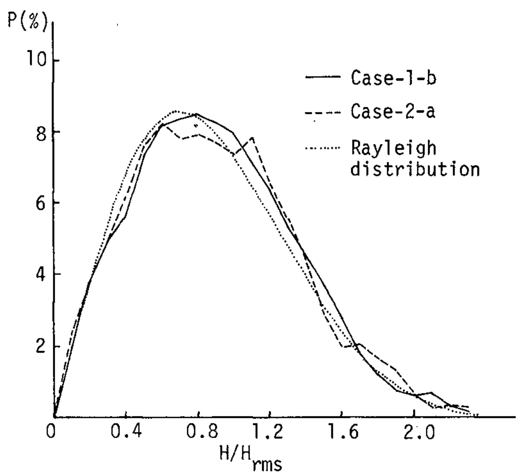


Fig-14 Wave height distributions defined by zero-up-cross method